USING A PASSIVE FEEDBACK CONNECTION TO CONTROL LOW-FREQUENCY PRESSURE FLUCTUATIONS IN A WIND TUNNEL

Peter Waudby-Smith [*1], **Antrix Joshi** [†1], **Christopher Sooriyakumaran** [‡1], **Christoph Gabriel** [§2], **and Martin Grabenstein** [¶2]

[1]Aiolos Engineering Corporation, Etobicoke, ON, Canada
[2]BMW Group, Muenchen, Germany

Résumé

Les souffleries à jet ouvert souffrent souvent de fluctuations de pression à basse fréquence et à forte amplitude, liées aux modes résonants du circuit. Généralement, ces fluctuations sont contrôlées à l'aide de générateurs de tourbillons de tuyères, de résonateurs de Helmholtz, de la conception des collecteurs, de l'annulation active du bruit et de diverses autres méthodes. L'objectif de cet article est d'évaluer une connexion de rétroaction passive (PFC) pour une utilisation dans une soufflerie aéro-acoustique. Le PFC peut réduire les fluctuations de pression à haute amplitude et basse fréquence dans le circuit de la soufflerie. En outre, le PFC peut également réduire les fluctuations non périodiques des vitesses du vent, c'est-à-dire les fluctuations de pression non associées aux modes résonants. Le PFC a obtenu ces résultats sans modifier de manière significative le gradient de pression statique axiale dans la soufflerie.

Mots clefs : Fluctuations de la pression en soufflerie, Connexion de rétroaction passive, Modèle de soufflerie

Abstract

Open jet wind tunnels often suffer from low-frequency, high-amplitude pressure fluctuations which are related to resonant modes within the circuit. Typically, these fluctuations are controlled using nozzle vortex generators, Helmholtz resonators, collector design, active noise cancellation, and various other methods. The goal of this paper is to evaluate a Passive Feedback Connection (PFC) for use in an aero-acoustic wind tunnel. The PFC can reduce the high-amplitude low-frequency pressure fluctuations in the wind tunnel circuit. In addition, the PFC can also reduce non-periodic fluctuations in wind speeds, i.e. pressure fluctuations not associated with resonant modes. The PFC achieved these results without significantly altering the axial static pressure gradient in the wind tunnel.

Keywords: Wind tunnel pressure fluctuations, Passive Feedback Connection, Model Wind Tunnel

1 Introduction

Wind tunnels are an important tool for the development of new vehicles. Automotive companies perform extensive aerodynamic, aero-acoustic and thermal testing on new vehicles to bring about improvements in efficiency, comfort, safety, and to show compliance with government regulations. With its combination of an open jet representing the unbounded free flow and solid floor representing the ground, the 3/4th open jet test section is the most common configuration in aero-acoustic wind tunnels, preferred for its open access to the test vehicle and its avoidance of near-field acoustic boundaries. When the air flow exits the nozzle, it interacts with the low-speed air in the plenum. As a result, a shear layer develops around the core of the jet between the nozzle and the collector. Small-scale vortex structures originate from the trailing edge of the nozzle, which are transported downstream towards the collector at approximately 65% of the velocity

of the jet [1]. These vortical structures evolve as they move downstream, which changes their associated frequencies. If the frequencies of these vortices match the resonance frequencies of any of the modes of the wind tunnel, high amplitude pressure fluctuations can be created.

There are four possible resonant conditions which can exist inside an open-jet closed-circuit wind tunnel [1–3].

— The complete wind tunnel circuit can resonate with frequencies associated with organ pipe modes.
— The vortices generated from the edge of the nozzle can impinge on the collector, which can send a pressure disturbance upstream. This pressure disturbance can generate additional vortices, setting up an edge-tone feedback loop.
— The volume within the test section plenum can resonate.
— The combination of the nozzle and the test section plenum can act as a Helmholtz resonator, causing a resonance.

The low-frequency high-amplitude pressure fluctuations can degrade the quality of aerodynamic and acoustic measu-

---
*. PeterW@aiolos.com
†. Antrix@aiolos.com
‡. Christopher@aiolos.com
§. Christoph.JO.Gabriel@bmw.de
¶. Martin.Grabenstein@bmw.de

rements in the wind tunnel and therefore must be minimized. Typically, a wind tunnel will be designed with several features or devices to minimize the pressure fluctuations. This is achieved by altering the strength and frequencies of the vortical structures in the flow, or by changing the geometry of the wind tunnel to passively target the resonant modes.

Several methods of controlling the low-frequency pressure fluctuations have been investigated. Passive control of the pressure fluctuations can be achieved by installing angled-blade vortex generators on the lip of the nozzle. The vortex generators are effective in breaking up large coherent vortex structures. However, they generate smaller vortical structures which produce high frequency noise. They also induce a vena-contracta type flow at the exit of the nozzle which produces a negative axial pressure gradient. These two factors make the use of angled-blade vortex generators unsuitable for application in many aerodynamic and aero-acoustic wind tunnels. In contrast, Blumrich et.al. [4] have developed a different vortex generator design which largely avoids the pressure gradient and noise contributions.

Rennie [1] investigated the effect of jet length on the low-frequency pressure fluctuations. The length of the jet in a pilot wind tunnel was varied by inserting spacers between the test-section diffuser inlet and the collector flaps. It was found that at a given wind speed, the jet pulsations frequencies were found to scale with the jet length. As the jet length is increased, the thickness of the downstream shear layer increases, which increases the turbulent energy. The amplitudes of the pressure fluctuations can be significantly reduced by selecting the 'correct' jet length, which is usually small. In practice, this is difficult to implement since the length of the test section is designed to suit the size of the intended test objects, and it is desirable to have the longest possible test section length.

Rennie [1] also investigated a collector design for the minimization of pressure fluctuations by using simple, rectangular flaps with bell-mouthed leading edges. It was found that the amplitude of the pressure fluctuations was sensitive to the collector inlet area. A larger collector was found to reduce the coefficient of overall unsteady pressure fluctuations ($C_{p,rms}$). A similar observation was also reported by Kudo et al. [5] and Wiedemann et al. [6] who found that the aerodynamic noise decreased when the collector area was increased. Kudo et al. however noted that increasing the collector area increases the pressure loss in the wind tunnel circuit. Therefore, the noise reduction from increasing the collector area should be weighed against the increased power demands from the main fan. The change in the geometrical shape of the collector can also have an impact on the pressure fluctuations. Such geometrical changes include modifying the collector wall angle, collector flap angle, collector leading edge geometry, changing the gap between the collector flaps and the diffuser. Changing any of the above aspects of the collector design may also have an impact on the axial static pressure gradient, and care must be taken during the collector design process to balance all the requirements of a wind tunnel.

Helmholtz resonators have been used successfully to attenuate pressure fluctuations arising from the coupling of the shear layer vortex frequencies and resonant modes in the circuit or test section [2, 7–9]. A Helmholtz resonator is comprised of a cavity with a neck connected to it. When a Helmholtz resonator is excited, the volume of fluid within the neck oscillates while the pressure of the fluid within the cavity fluctuates at a certain frequency. The absorption of sound within the resonator occurs due to various mechanisms. There are viscous losses along the neck, as well as along the front wall of the resonator. There are also thermal losses at the wall of the resonator cavity. There may also be some non-linear losses due to circulation effects and turbulence, specially in the presence of very high sound intensities. [10, 11]

The sizing of resonators follow the theoretical and experimental background provided by Ingard [11], Selamet and Lee [12] and others [13–15]. The key parameter is the natural frequency of the resonator, which is given by $f = \frac{c}{2\pi}\sqrt{\frac{S}{(l+\delta)V}}$. Here, f is the tuning frequency of the resonator, c is the speed of sound, S is the area of the neck, l is the length of the neck, δ is an adjustment to the neck length which is equal to 0.85 x the neck diameter, and V is the cavity volume. The relatively narrow bandwidth of these devices means that several resonators tuned to different frequencies can be required.

A Helmholtz resonator can be connected to the wind tunnel airline at the plenum or elsewhere in the circuit. To deal with a resonant mode, the resonator should ideally be connected at the location of the anti-node where the velocity of the oscillation is largest; though this location is not straightforward to determine. A full-scale wind tunnel has numerous constraints on the resonator location and sizing due to architectural needs, other sub-systems, and geometrical constraints. As a result, the resonators considered for the full-scale wind tunnel have shapes and locations which are not typically represented in the literature. Therefore, model-scale testing is often used to characterise the effectiveness of the resonators before they are implemented in the full-scale tunnel.

Beland [7] also investigated the use of a pressure compensation channel to reduce the low-frequency pressure fluctuations. When a standing wave is established in the wind tunnel circuit (which causes pressure fluctuations), there are fixed locations of maxima and minima (or nodes and anti-nodes) in the sound pressure. By connecting these nodes and anti-nodes of pressure with a duct, the overall sound power associated with the standing wave can be decreased. With the decrease in the strength of the standing wave, the activation mechanism of vortex generation in the edgetone feedback is damped, which reduces the strength of the resonance in the wind tunnel. Beland [7] found that the standing wave had a node right before corner 1 (the corner immediately downstream of the test section), while the anti-node was present in the test section. By connecting these two locations with an external compensation channel, the overall $C_{p,rms}$ levels were decreased. It was noted that the compensation channel chan-

ged the static pressure distribution in the vicinity of the collector. To correct the pressure distribution, the collector angle had to be increased by $10°$. The size and the form of the compensation channel opening close to corner 1 had a great influence on the performance of the device, while the opening in the test section chamber played a subordinate role. The compensation channel concept was ultimately not implemented in the full-scale tunnel at FKFS to avoid making expensive structural changes to the wind tunnel building.

Another similar technique was used by Wang et al. [9] in a model scale wind tunnel at Tongji University by using the principle of sound wave interference. One end of a pipe was connected to the test section. At some distance along the length of the pipe, an interlink was made with the wind tunnel airline, creating two pipe segments. As an incident sound pressure field hits the open end of the pipe in the test section, some of the energy is transmitted into the pipe, while some energy is reflected off the open end, as well as from the end of the pipe. The properties of the pressure field coming out of the interlink can be determined by fixing the length of the two segments. The incident pressure field can then be attenuated by using destructive interference from the interlink pressure field. It was found that the sound interference method decreased pressure fluctuations in certain frequency bands, while increasing them in other bands.

Wickern et al. [3] used a $1/20^{th}$ scale pilot wind tunnel to investigate the use of an Active Resonance Control system (ARC). Real time measurements of the pressure fluctuations were made using a microphone located in the test section. The phase of the measured signal was shifted, and it is played back through a loudspeaker placed in the return leg of the wind tunnel such that the pressure fluctuations could be attenuated. When the ARC system was implemented in the full-scale Audi aero-acoustic wind tunnel, 23 dB, 20 dB, and 15 dB reductions in the sound pressure levels (SPL) of resonances at 2.4 Hz, 3.9 Hz, and 6.8 Hz were found. The benefit of the ARC system is that a single space efficient system can dampen pressure fluctuations at multiple frequencies.

Many other devices and techniques have been extensively studied by many researchers. The current paper, like the approaches taken in [7,9], considers a geometry change whereby a passive feedback connection between the first cross-leg and the test section plenum within the circuit is used to alter these low-frequency pressure fluctuations. The duct sets up a passive feedback mechanism to attenuate the low-frequency high-amplitude pressure fluctuations.

2 Test setup

Aiolos has found that the optimization of a wind tunnel circuit to minimize low-frequency pressure fluctuations is best performed in conjunction with wind tunnel tests rather than relying only on analytical or finite element methods, particularly when design constraints limit the application of previously successful geometries. Scale model tests with a full-circuit Model Wind Tunnel (MWT) have been used to effectively identify and correct low-frequency pressure fluctuations

present in a full-scale tunnel [16]. The magnitudes of the fluctuations generally match between full and model scale, while the frequencies scale linearly with the geometrical scale of the MWT. This approach was taken in the development of a new aero-acoustic wind tunnel for BMW, leading to a test program using a $1/10^{th}$ scale MWT of the planned full-scale facility.

For the design of the BMW full-scale tunnel, only passive approaches were considered. This is because passive devices (resonators and PFC) are mechanically simple with no moving parts. Once they are tuned correctly, they can be expected to always function without failure. The downsides of using a passive approach are the large volume requirement for the resonators, especially for the control of low-frequency fluctuations, and the complications of tuning such large devices. In the case of the BMW wind tunnel the tuning was addressed with reduced scale model wind tunnel tests.

Since the interest for these tests was related to a full-scale automotive aero-acoustic wind tunnel, the values given in this paper are generally converted to their equivalent full-scale values. This scaling was applied using the 1:10 scale factor on frequency and length dimensions; the wind speeds were not scaled.

A 3D rendering of the MWT is shown in Figure 1. The MWT was a close geometrical representation of the planned full-scale circuit but without any acoustic treatment except in the fan region. The $3/4^{th}$ open jet test section had a nozzle size of 0.4 m x 0.625 m. At the end of the test section, a collector with bell-mouth inlet leading edge was used to divert the flow into the diffuser. Four large resonators with variable geometry were included in the model scale tunnel. The volume of the resonators could be modified, as well as the geometry of the connection between the resonators and the wind tunnel circuit. The resonant frequencies of resonators 1, 2 and 4 were between 1.2 Hz to 1.8 Hz. These three resonators were counteracting the dominant second organ pipe mode within the full-scale circuit, which is approximately 1.6 Hz. Resonator 3 was tuned to counteract resonance around 3.2 Hz, which corresponded to the fourth organ pipe mode. The MWT included a connection path between the first cross-leg (located downstream of the first corner) to the rear wall of the test section plenum, termed the Passive Feedback Connection (PFC). The influence of the PFC on the pressure fluctuations in the tunnel is the subject of this paper.

2.1 Determination of $C_{p,rms}$

The low-frequency pressure fluctuations in the MWT were measured with a GRAS Type 40 AN microphone and GRAS Type 26 AK preamp located out-of-flow at a location equivalent to mid-length and the height of a car in the full-scale test section. This arrangement provided a ± 1 dB response down to 1 Hz and ± 2 dB down to 0.5 Hz (which are 0.1 Hz and 0.05 Hz equivalent full-scale). A foam wind screen was used to reduce the self-noise of the microphone. The pressure signal was recorded at a sampling rate of 800 samples/s for 300 seconds. The signal was converted to the frequency domain
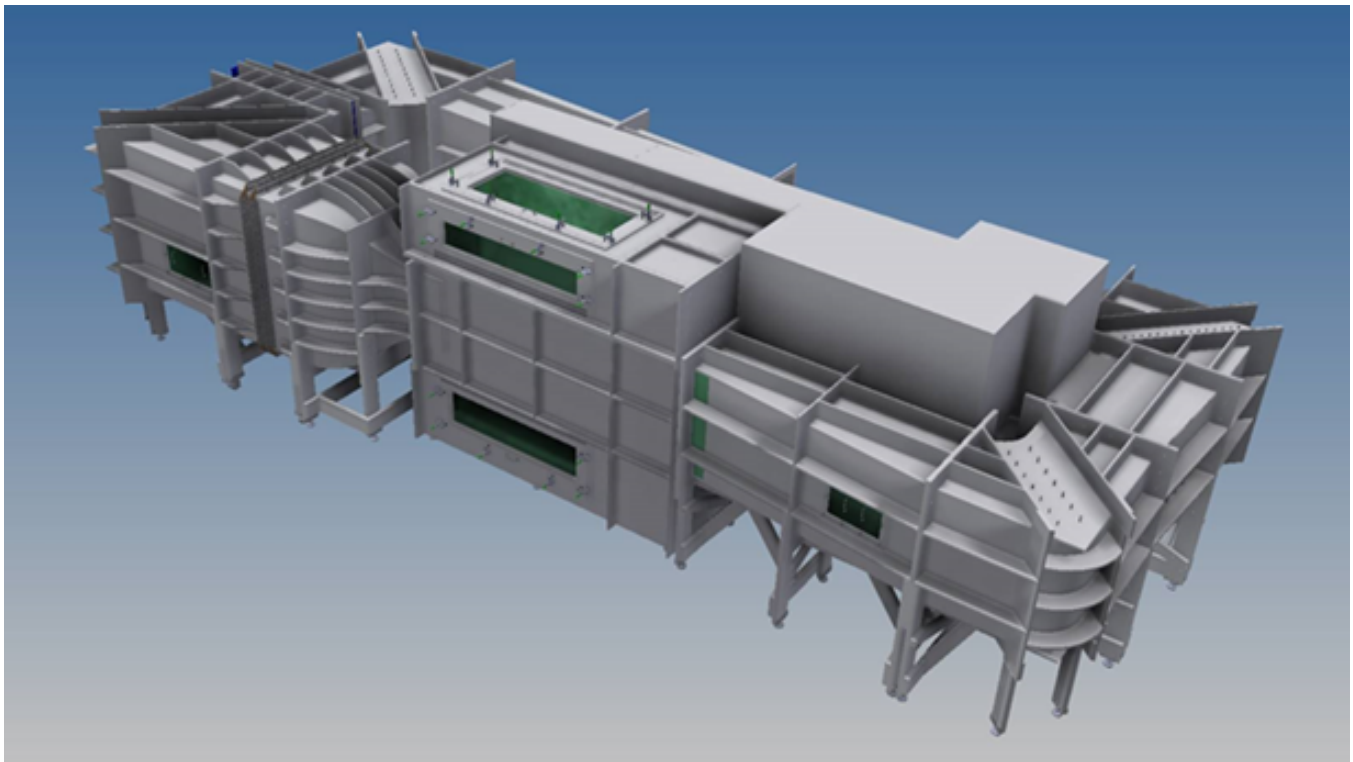
Figure 1: A 3D rendering of the model wind tunnel (MWT)

with 12801 intervals and a 312.5 Hz bandwidth by breaking the time-series into 7 non-overlapping segments, leading to a frequency interval of 0.024 Hz (0.0024 Hz equivalent full-scale) for each segment. A Hanning windowing function was applied to reduce the spectral leakage with the Hanning window correction applied to obtain the correct amplitude of the pressure power spectrum. The seven spectra were combined using rms averaging. Overall $C_{p,rms}$ values were determined by integrating the spectral $C_{p,rms}$ distribution over the full-scale frequency range of 1 Hz to 20 Hz, and were the primary measure of the low-frequency pressure fluctuations in the test section. The sound measurements reported in the paper are not weighted (i.e. flat response) over the full frequency range.

2.2 Wind speed measurements

The test section wind speed was inferred by measuring the pressure drop across the contraction. The pressure drop was measured using a Scanivalve differential pressure scanner (model DSA3217 16Px) connected to two pneumatically averaged static taps installed in the settling chamber downstream of the flow conditioning devices, and two pneumatically averaged static taps in the plenum. These contraction pressure drops were correlated to the actual wind speeds in the test section by first calibrating the wind tunnel with a bent-stem Pitot-static probe located at the equivalent vehicle center location. The pressure scanner sampled the pressure at 10 Hz, equivalent to 1 Hz full-scale. The time series results from these measurements were used to determine the *wind speed variability* and *unsteadiness* over the duration of a test.

2.3 Axial static pressure gradient measurements

The axial static pressure gradient was measured using a single bent-stem Pitot-static probe which was traversed at a low speed over the axial length of the test section. The axial pressure gradient was obtained by fitting an appropriate order polynomial to the pressure coefficient data and differentiating the curve fit equation to obtain the local gradient.

2.4 Passive Feedback Connection (PFC)

A sketch of the MWT circuit is given in Figure 2, which shows the layout of the four resonators in the circuit, along with the passive feedback connection. The Resonator 1 was closed for all the cases shown in this paper. The necks of Resonators 2, 3, and 4 were connected to the return cross leg, test section diffuser, and the rear wall of the plenum respectively. The passive feedback connection was created by attaching a duct between the return cross leg and Resonator 4.

3 Results

An extensive test program was undertaken to determine the geometries of Resonators 2, 3, and 4, as well as the geometry of the collector, in order to minimize the pressure fluctuations and axial static pressure gradient. The effectiveness of the PFC was investigated with these optimized geometries already configured. The PFC operated through the volume of the Resonator 4, and it was not possible to isolate the PFC from Resonator 4. The results from the five configurations listed in Table 1 illustrate the performance of the PFC. Progressing from case A to C1, the Resonator 4 and the PFC
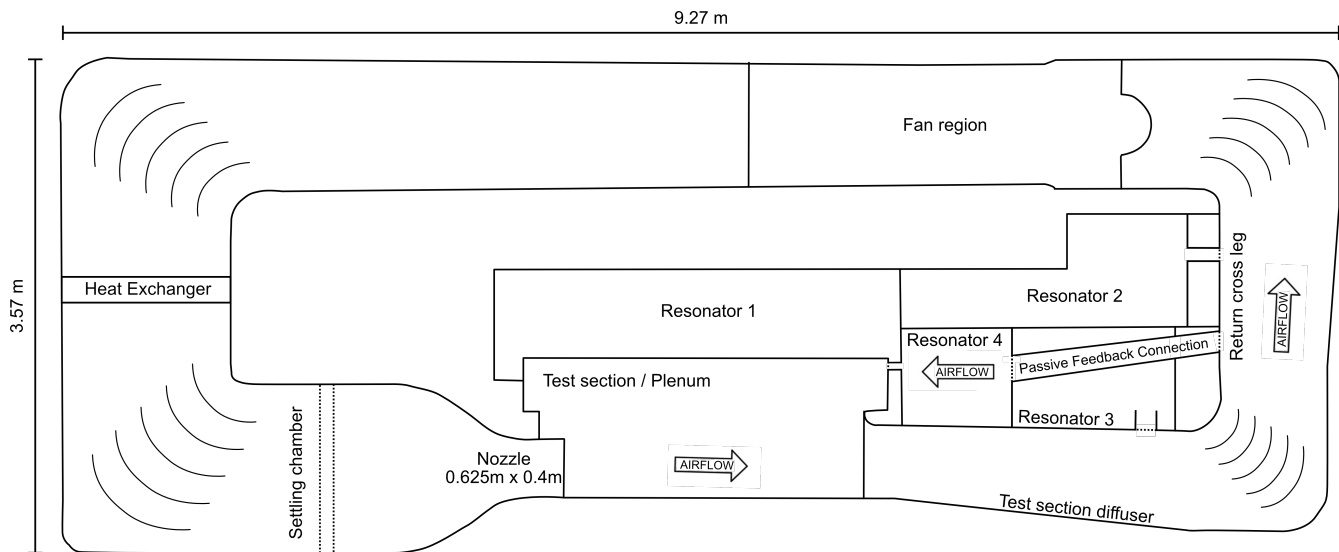
Figure 2: A sketch of the circuit showing the layout of the resonators and the passive feedback connection

Table 1: Resonator and PFC configurations

Name	Res. 1	Res. 2	Res. 3	Res. 4	PFC	PFC flow rate (Q_{pfc}/Q_{ts})
Case A	closed	open	open	closed	closed	0.0%
Case B	closed	open	open	open	closed	0.0%
Case C1	closed	open	open	open	open	3.0%
Case C2	closed	open	open	open	open	5.1%
Case C3	closed	open	open	open	open	6.5%

are systematically opened, while keeping the rest of operating conditions the same. Progressing from case C1 to C3, the flow rate through the PFC was systematically increased. The arrangement of the collector was kept the same for all five cases. The flow rate through the PFC duct (Q_{pfc}) was measured and related to the flowrate through the test section (Q_{ts}). The flow rate of air through the PFC could be varied by changing the inlet area of the PFC duct at the cross-leg.

The overall normalized out-of-flow unsteady static pressure measurements, $C_{p,rms}$, are shown in Figure 3. The baseline case (Case A, red circles in Figure 3) had the worst $C_{p,rms}$ amongst the configurations presented here at all wind speeds, peaking at 128 kph. The driver of this pressure fluctuation was a relatively small peak at 1.6 Hz, which is associated with the 2nd organ pipe resonance mode. It should be noted that the baseline case is not that of a wind tunnel with no resonators. The Resonators 2 and 3, as well as an optimized collector had already created conditions of low levels of pressure fluctuations for case A. By opening Resonator 4 (case B, blue square in Figure 3), the $C_{p,rms}$ values were further decreased. Further reduction could be achieved by opening the PFC up to a flow rate of $Q_{pfc}/Q_{ts} = 3.0\%$ (case C1, green diamonds in Figure 3). At higher flow rates, the gains made by using the PFC were diminished and the $C_{p,rms}$ values increased. The $C_{p,rms}$ for the highest flowrate case C3 however were always lower than case A (no Resonator 4) at all wind speeds. It is postulated that at higher flow rates, the flow through PFC began

degrading the performance of Resonator 4, which led to an increase in the overall $C_{p,rms}$ for cases C2 and C3 compared to case C1. A resonator operates by oscillating a finite amount of a fluid inside the neck, with the large volume acting as a spring-mass-damper system. Since the PFC is connected to the Resonator 4, by increasing the flow rate inside the PFC (and thus the resonator), the effectiveness of the resonator is hindered. Consequently, the benefit of the PFC is outweighed by the loss in effectiveness of the resonator.

Beland [7] had noted that the effectiveness in the suppression of the pressure fluctuation was sensitive to the geometry of the inlet region for the compensation channel. The shape and the size of the outlet of the compensation channel into the test section plenum was inconsequential. A long, narrow opening in the plenum chamber wall, which was minimized to around 9% of the nozzle surface area was used by Beland [7]. In the current investigation, the outlet geometry of the PFC was found to also have an impact on the performance, but this is likely also due to its effect on the Resonator 4 performance.

The effectiveness of the PFC was further investigated by examining the wind speed time traces obtained though the pressure measurements. Figure 4 shows normalized wind speed traces for cases A to C1 at a nominal wind speed of 120 kph. The time shown on the x-axis has been corrected to full-scale tunnel values by multiplying it by the geometrical scaling factor. A 10 second (full-scale) rolling average of
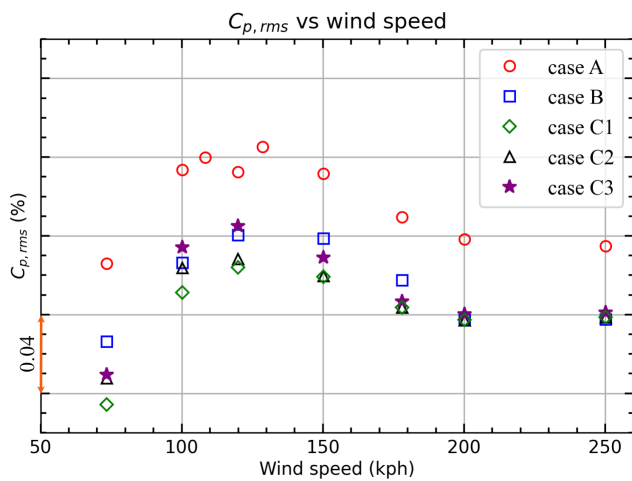
Figure 3: Overall $C_{p,rms}$ values versus the wind speed for the five cases ($1\ Hz \leq f \leq 20\ Hz$ full-scale).

the wind speed ($\hat{ws}$) is applied to remove any short-term fluctuations. The rolling averaged wind speed ($\hat{ws}$) data is then normalized by the mean wind speeds ($\bar{ws}$), and the results are plotted as shown in Figure 4. That is, *wind speed variability* = ($\frac{\hat{ws}}{\bar{ws}} - 1$). Unsteadiness in wind speed is evident for the cases without PFC by observing Figures 4 (a) and (b) where during intermittent spikes, the wind speeds reached *wind speed variability* = -0.7% and -0.8% respectively. With the PFC open (case C1), the intermittent large spikes were not observed, and the *wind speed variability* was very low.

Note that the MWT was operated with only a fan speed controller, which maintained a fixed fan rotational speed (i.e., a fixed volume flow rate of air). Small and slow drifts in the mean wind speed due to temperature drifts were accounted for with a straight-line fit to the measured data.
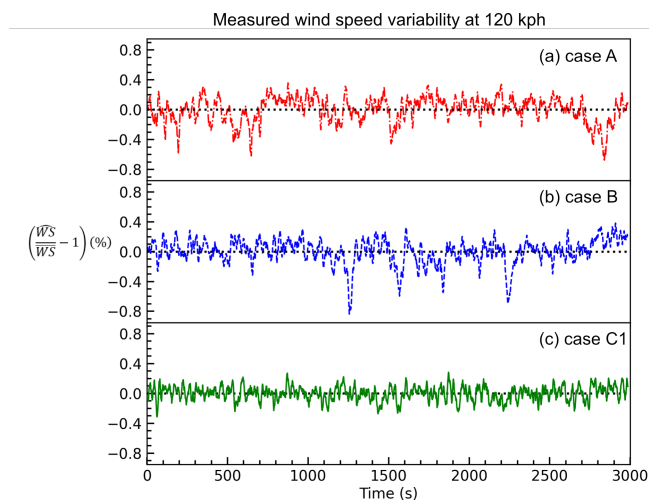

Figure 4: Wind speed variability demonstrated by normalized wind speed trace for cases A-C1 at nominal speed of 120 kph

An overall wind speed stability value can be deduced from the standard deviation of the wind speed time series. Results for different wind speeds are shown in Figure 5 which

shows *overall wind speed unsteadiness* $= \frac{\sigma(\hat{ws})}{\bar{ws}}$. Use of the PFC is shown to improve the *overall wind speed unsteadiness* values by almost a factor of 2 across the wind speed range. The data suggests that increasing the flow rate through the PFC can marginally improve the *overall wind speed unsteadiness*.
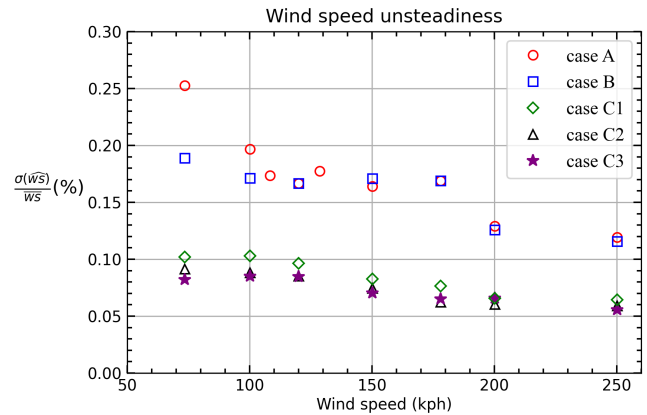

Figure 5: Overall wind speed unsteadiness for an averaging time of 10s (full scale)

This improvement in the wind speed unsteadiness is also evident by the improvements of the very low frequency pressure fluctuations ($f < 1\ Hz$). Spectra for the five test conditions converted to dB(Z) with frequency intervals of 0.1 Hz (full-scale equivalent) are shown in Figure 6. The use of the PFC is shown to have its strongest influence for $f < 1\ Hz$.
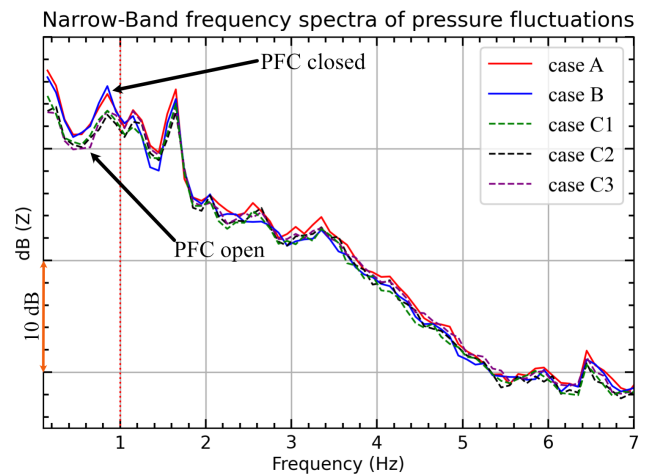

Figure 6: Narrow-band frequency spectra of pressure fluctuations at 120kph

A separate issue for wind tunnel test models is the variation of the axial static pressure due to the buoyancy force that can be induced on the test model by the pressure variation. It is desirable to have the smallest possible axial static pressure gradient in a wind tunnel test section. Figure 7 shows that the addition of a PFC (case C1) does not significantly alter the axial static pressure gradient in the MWT.
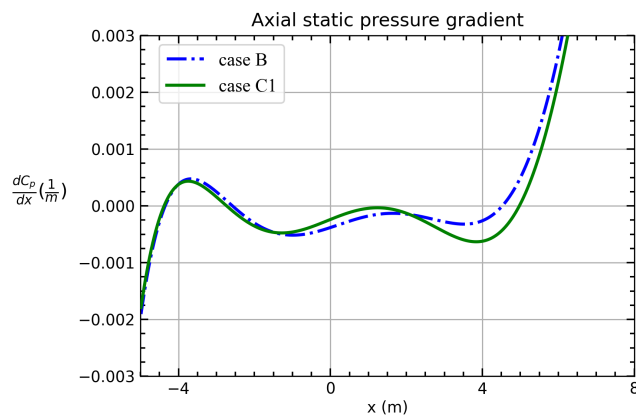
Figure 7: Axial static pressure gradients for cases B and C1

4 Conclusion

A $1/10^{\text{th}}$ scale model wind tunnel was developed to aid in the design of a new aero-acoustic wind tunnel for BMW. The model wind tunnel was used to optimize the collector design, as well as to tune the Helmholtz resonators. In addition to the traditional means of controlling the pressure fluctuations, another novel approach, the Passive Feedback Connection (PFC) was also tested, which is the concern of the paper. The PFC connected the return leg of the wind tunnel with a resonator which was connected to the test section plenum. At low flow rates through the PFC, reductions in the amplitudes of the low-frequency pressure fluctuations were found. At higher flow rates, the performance of the overall system was slightly diminished, presumably due to the degradation of the effectiveness of the resonator. The PFC was also found to significantly improve the wind speed stability in the wind tunnel. Without the PFC, non-oscillatory spikes in wind speed variability were observed. With the PFC connected, these spikes were eliminated. The PFC achieved these improvements in pressure fluctuations without compromising the axial static pressure gradient.

References

[1] Mark Rennie. Effect of jet length on pressure fluctuations in 3/4-open jet wind tunnels. In Motor Industry Research Association Vehicle Aerodynamics 2000 Symposium, 2000.

[2] Peter Waudby-Smith and Ramani Ramakrishnan. Wind tunnel resonances and helmholtz resonators. Canadian Acoustics, 35(1) :3–11, 2007.

[3] Gerhard Wickern, Wilhelm von Heesen, and Steffen Wallmann. Wind tunnel pulsations and their active suppression. SAE transactions, pages 1403–1416, 2000.

[4] Reinhard Blumrich, Nils Widdecke, Jochen Wiedemann, Armin Michelbach, Felix Wittmeier, and Oliver Beland. New FKFS technology at the full-scale aeroacoustic wind tunnel of university of Stuttgart. SAE International Journal of Passenger Cars-Mechanical Systems, 8(2015-01-1557) :294–305, 2015.

[5] Toshifumi KUDO, Kazuhiro MAEDA, and Masaharu NISHIMURA. Techniques of reducing aerodynamic noises in 3/4 open-jet wind tunnels. Journal of Environment and Engineering, 4(2) :276–288, 2009.

[6] Jochen Wiedemann, Gerhard Wickern, Bernd Ewald, and Christof Mattern. Audi aero-acoustic wind tunnel. Technical report, SAE Technical Paper, 1993.

[7] Oliver Beland. Buffeting suppression technologies for automotive wind tunnels tested on a scale model. In Proceedings of the 6th FKFS-Conference on Progress in Vehicle Aerodynamics and Thermal Management, Stuttgart, 2007.

[8] Joseph Yen, Edward Duell, Joel Walter, and Amir Kharazi. Caa study of helmholtz resonator application on edge-tone noise suppression. In 18th AIAA/CEAS Aeroacoustics Conference (33rd AIAA Aeroacoustics Conference), page 2103, 2012.

[9] Yigng Wang, Zhigng Yang, and Qilang Li. Methods to control low frequency pulsation in open-jet wind tunnel. Applied Acoustics, 73(6-7) :666–672, 2012.

[10] AI Komkin, MA Mironov, and AI Bykov. Sound absorption by a helmholtz resonator. Acoustical Physics, 63(4) :385–392, 2017.

[11] Uno Ingard. On the theory and design of acoustic resonators. The Journal of the acoustical society of America, 25(6) :1037–1061, 1953.

[12] Ahmet Selamet and Iljae Lee. Helmholtz resonator with extended neck. The Journal of the Acoustical Society of America, 113(4) :1975–1985, 2003.

[13] Chenzhi Cai and Cheuk Ming Mak. Acoustic performance of different helmholtz resonator array configurations. Applied Acoustics, 130 :204–209, 2018.

[14] Dan Zhao, Chris A'barrow, Aimee S Morgans, and Jon Carrotte. Acoustic damping of a helmholtz resonator with an oscillating volume. AIAA journal, 47(7) :1672–1679, 2009.

[15] Ruolong Ma, Paul E Slaboch, and Scott C Morris. Fluid mechanics of the flow-excited helmholtz resonator. Journal of Fluid Mechanics, 623 :1–26, 2009.

[16] Mark Rennie, Moo-Sang Kim, Jung-Ho Lee, and Jung-Do Kee. Suppression of open-jet pressure fluctuations in the hyundai aeroacoustic wind tunnel. SAE transactions, pages 404–418, 2004.